JACS
JOURNAL OF THE AMERICAN CHEMICAL SOCIETY
pubs.acs.org/JACS
Communication

Motor and Rotor in One: Light-Active ZnO/Au Twinned Rods of Tunable Motion Modes

Sinan Du, Huaguang Wang, Chao Zhou, Wei Wang,* and Zexin Zhang*

Cite This: J. Am. Chem. Soc. 2020, 142, 2213−2217
Read Online
ACCESS | Metrics & More | Article Recommendations | Supporting Information

ABSTRACT: Precise control of the motion of micromachines is the key to achieving their functions for practical applications. The main challenge is that a given micromachine can typically exhibit only one motion mode, i.e., translation or rotation, while having multiple modes of motion resulting from a simple actuation is still rare. Here we designed and synthesized photochemically powered zinc oxide/gold (ZnO/Au) rods that exhibit multiple motion modes. Under homogeneous UV irradiation, these ZnO/Au rods undergo a transition from ballistic motion to persistent rotational motion upon increasing the fuel concentration or the light intensity. In addition, the rods can switch modes from a circular motion to a helical motion and then a straight-line motion by tuning the angle of incident light. We envision that such attractive colloidal micromachines with controllable motions hold considerable promise for diverse practical applications.

Colloidal micromachines that convert energy from their surroundings into mechanical motion[1−14] have attracted increasing attention due to their promising potential applications in biomedicine,[15,16] environmental remediation,[17,18] biochemical sensing,[19] etc. As a common type of micromachines, motors exhibit mainly translational motion,[2,3] while rotors move predominantly in circles.[20−23] Most of the recent research on micromachines has focused on motors. For example, platinum/gold bimetallic rods[3,24] and TiO_2−Au spheres[25] exhibit a translational motion that is desired in transportation tasks, such as cellular delivery and drug loading and release. In contrast, rotors have received relatively little attention due to their low yield and more difficult fabrication processes. Rotational motion is usually achieved based on geometrically asymmetric active particles that produce a torque on the particle's center of mass.[21−23,26−29] Previous studies have shown that rotors are indispensable in many applications, including microdrillers,[22,30] microstirrers,[10,31] and model systems for soft matter physics.[27] In particular, rotors are more powerful when moving through viscous biological media, such as vitreous gel, stomach mucus, and intestinal fluids.[15,32−34] Generally, micromachines under specific actuation have only one dominant mode of motion, either translation or rotation, thus limiting the range of their applications. Combining various motion modes in one micromachine is highly desirable for modulating functions "on the fly", which may eventually make multifunctional micromachines a reality.

Here we demonstrate that asymmetric ZnO/Au Janus micromachines (hereinafter referred to as ZnO/Au rods) can experience a transition from ballistic motion to persistent rotational motion upon increasing the fuel concentration or the light intensity. Moreover, the rods change from a predominant rotation to a linear motion by modulating the incident angle of the light. The fuel- and light-tunable motion modes of ZnO/Au rods afford a "motor and rotor in one" micromachine, which holds considerable promise in applications where translational and rotational motions are simultaneously required.

To realize multiple motion modes, we designed a photochemically powered micromachine, based on ZnO "twinned" rods with two segments of different diameters, which are further coated with a gold layer on one side (Figure 1b−e; see also Supporting Information, Figures S1−S3). Such a rod undergoes self-electrophoresis when illuminated by UV light in H_2O_2 (Figure 1a), similar to that of TiO_2−Au micromotors.[25] The driving force of the motion originates from a self-generated electric field due to the asymmetric distribution of protons during the photocatalytic reaction of H_2O_2. This force, being perpendicular to the rod's major axis, induces a torque on a rod with two segments of different diameters, which induces rotation of the rod.[27]

To test the self-electrophoresis mechanism, numerical simulations and particle image velocimetry (PIV) experiments were carried out. We found, by finite element simulations (COMSOL Multiphysics), that the electrical potential (Figure 1f) is higher near the ZnO side than the Au side, and the electric field points from the anode (ZnO side) to the cathode (Au side). Thus, the rod should move toward the ZnO side, which in turn creates fluid flow in the reverse direction (Figure 1g). To visualize and verify experimentally the flow field, a ZnO/Au rod was fixed on a glass substrate, and the movements of tracers around the rod were analyzed by PIV.[35] The instantaneous velocity vectors of the tracers show a pattern (Figure 1h) similar to that in Figure 1g, confirming the

Received: December 5, 2019
Published: January 20, 2020

https://dx.doi.org/10.1021/jacs.9b13093
J. Am. Chem. Soc. 2020, 142, 2213−2217

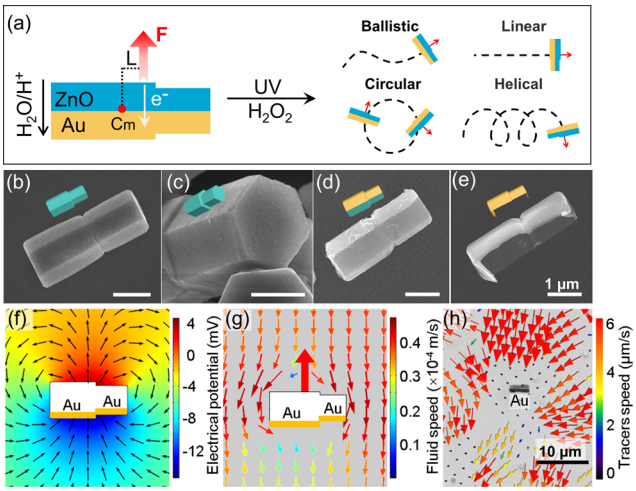

Figure 1. Design of motor/rotor from ZnO/Au rods. (a) Self-electrophoresis mechanism of a ZnO/Au rod and its four motion modes. SEM images of (b) a ZnO rod, (c) a cross-section of the ZnO rod, (d) a ZnO/Au Janus rod, and (e) a residual Au shell after removal of ZnO by hydrochloric acid. (f) Simulated electrical potential (color-coded) and electric field (arrows) distribution around a ZnO/Au rod. (g) Simulated flow velocity (color-coded) and flow field (arrows). (h) Experimentally measured instantaneous velocity vectors of PS tracers around a fixed ZnO/Au rod by particle image velocimetry. Arrows and colors indicate directions and magnitudes of flow, respectively.

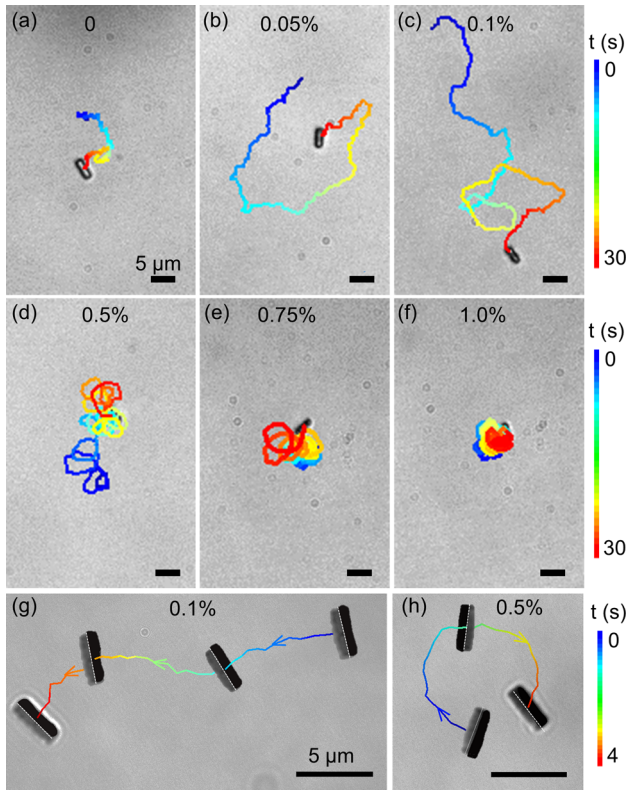

Figure 2. Effect of H_2O_2 concentrations on the motion modes of ZnO/Au rods. Representative trajectories of ZnO/Au rods moving at varying H_2O_2 concentrations with UV intensities of 32 mW/cm^2: (a) 0, (b) 0.05%, (c) 0.1%, (d) 0.5%, (e) 0.75%, and (f) 1.0% v/v. Superimposed time-lapse snapshots and corresponding complete trajectories of ZnO/Au rods moving in (g) 0.1% and (h) 0.5% H_2O_2. Note that the direction of motion is pointing from the Au side (dark) to the ZnO side (gray). Scale bars: 5 μm.

propulsion mechanisms (see also Supporting Information, Figure S4).

The dynamics of the ZnO/Au rod is found to heavily depend on the fuel (H_2O_2) concentration, shown in Figure 2a–f (also see Supporting Video S1). At low fuel concentrations (0.05–0.1%), the trajectories resemble most reported spherical Janus micromotors displaying ballistic motion (Figure 2b,c), in contrast to the slow Brownian motion in pure water (Figure 2a). The direction of the motion changes stochastically due to thermal fluctuations, consistent with previous work.[13,27] At intermediate fuel concentration (0.5%), the particles show a spiral-like trajectory (Figure 2d). With further increasing fuel concentration (0.75–1.0%), circular trajectories are observed (Figure 2e,f). Such circular orbits are due to the deviation of the increased propulsion force from the mass center of the rods, which generates a torque on the particle.[36−38] These observations suggest that the motion modes may be modulated by adjusting the H_2O_2 concentrations. Moreover, adjusting the UV light intensity has a similar modulation effect on the motion modes (Supporting Information, Figure S5).

To observe the details of the translation and rotation, high-magnification bright-field micrographs with enhanced contrast were examined. Specifically, ballistic translational motion generated a trajectory with random reorientation (Figure 2g), while the rotational motion yielded a circular trajectory with periodic reorientation (Figure 2h). The trajectories of the motion confirm that the particles are propelled in a direction perpendicular to the major axis of the rods with the ZnO side facing forward.

To quantify the dynamics of the ZnO/Au rods, the translational velocity (v), angular velocity (ω), curvature (κ), and mean-squared angular displacements ($\langle\Delta\theta^2\rangle$) were calculated. In pure water, the rods undergo Brownian motion, and θ changes randomly due to thermal fluctuations (Figure 3a).[36,39] In contrast, at high H_2O_2 concentration, θ exhibits periodicity with time, signifying the circular motion of the particle (Figure 3b). This is also confirmed by the change of the curvature, κ. The curvature fluctuates around zero in pure water (Figure 3 c) but holds a constant nonzero value at high H_2O_2 concentrations (Figure 3d). In addition, due to the enhanced self-electrophoretic effect at high H_2O_2 concentration, the velocities, v and ω, increase with increasing H_2O_2 concentration (Figure 3e). Moreover, $\langle\Delta\theta^2\rangle$ changes from a free diffusion (slope = 1) to a superdiffusion mode (slope = 2) with increasing H_2O_2 concentration (Figure 3g), further confirming the change of motion mode with changing H_2O_2 concentration. These quantitative analyses imply that the rods exhibit elongated trajectories with less rotation at low H_2O_2 concentration and "tight circular" trajectories with high angular velocity at high H_2O_2 concentration, which is consistent with the observations in Figure 2.

The question then arises: Why do ZnO/Au rods move in circular trajectories? Previous studies have shown that the geometric asymmetry of the particle plays a key role in inducing rotational motion.[34,36,37] To explore the mechanism of rotation for ZnO/Au rods, control experiments were performed on ZnO/Au rods with uniform diameter as opposed to the twinned rods with two segments of different diameters. No circular motion of the uniform diameter rods is observed, regardless of the H_2O_2 concentration (Supporting Information,

https://dx.doi.org/10.1021/jacs.9b13093
J. Am. Chem. Soc. 2020, 142, 2213−2217

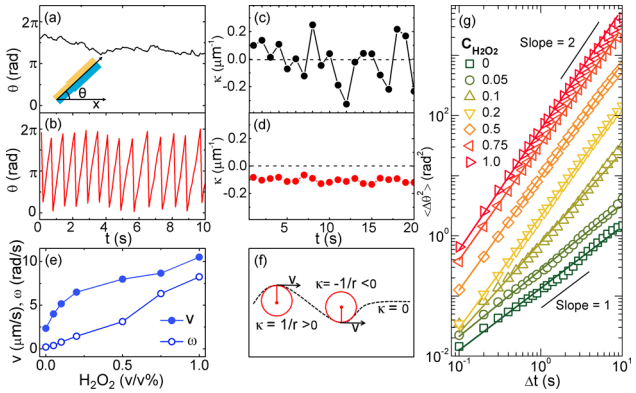

Figure 3. Dynamics of ZnO/Au rods under various H_2O_2 concentrations. Time evolution of angle θ for the ZnO/Au rods in (a) pure water and (b) 1% H_2O_2. Inset: θ defined as the orientation of the rod with respect to the x axis of the analyzed frame. The curvature κ for the ZnO/Au rods is shown in (c) pure water and (d) 1% H_2O_2. κ is defined as the inverse of the radius of its osculating circle (red circles) at each point (f). (e) Linear velocity (v) and angular velocity (ω) of the ZnO/Au rods as a function of H_2O_2 concentrations. (g) Mean-squared angular displacements ($\Delta\theta^2$) for ZnO/Au rods at different H_2O_2 concentrations. Error bars are smaller than the data points.

Figure S7). These observations provide strong evidence that the circular motion is a consequence of the asymmetric shape of the twinned rods.

In general, for a photosensitive semiconductor material like ZnO, the orientation of incident light has a strong impact on the motion.[7] Indeed, it has been proposed that isotropic TiO_2 microspheres can "swim" away from a light source; this is the so-called negative phototaxis behavior.[7] Based on this principle, here we found an alternate way to modulate the motion of the rods, i.e., by tuning the angle (α_z) of the incident light with respect to the plane of the motion. With increasing α_z, the circular trajectories gradually transformed into linear ones (Figure 4). For example, helical ($\alpha_z = 45°$) and straight-line ($\alpha_z = 90°$) trajectories were observed (Figure 4d–f and Supporting Video S2).

To rationalize the phototaxis motion of the ZnO/Au rods, we analyzed the forces and the resulting torque generated on the rod when changing the angle of the incident light. The rods exhibit positive phototaxis motion, with the ZnO side facing the light source and moving toward the direction of illumination. For a light field where the incident light is perpendicular to the plane of motion ($\alpha_z = 0°$), the propulsion force is always perpendicular to the major axis of the particle (Figure 4g). The torque is thus maintained, resulting in persistent rotational motion.[27] However, for an incident light that is parallel to the plane of motion ($\alpha_z = 90°$), the propulsion force depends on the orientation of the rods because the photocatalytic reactions occur only on the irradiated side.[7] Quantitatively, the torque can be expressed as $T = FL \cos \beta$, where F is the propulsion force, L is the effective lever arm, and β is the angle between the minor axis of the rods and the direction of the force (Figure 4h). When β increases, the torque decreases, so that rotation is prohibited and the motion changes to translation. For intermediate angles of incidence ($0 < \alpha_z < 90°$), the rods were propelled by two forces: one is perpendicular to the major axis of the particle (Figure 4g), and the other is toward the light source (Figure 4h), leading to the helical trajectories in Figure 4c–e.

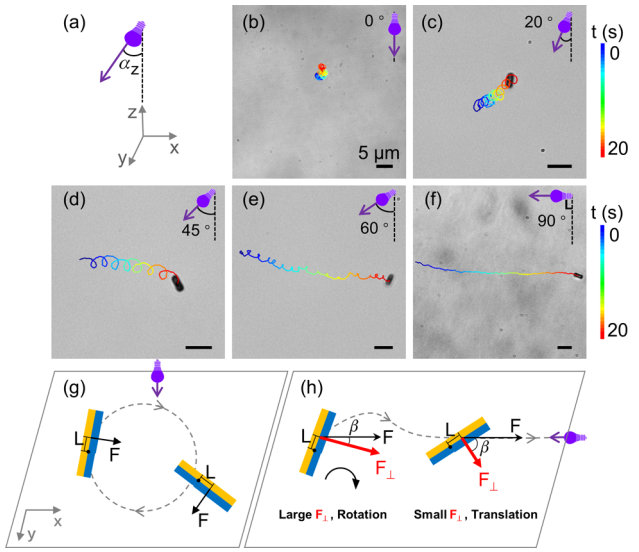

Figure 4. Orientation of incident light dictates the modes of motion of ZnO/Au rods. (a) Schematic of angles of incidence with respect to the z axis, α_z. Trajectories of ZnO/Au rods under irradiation at various α_z: (b) 0°, (c) 20°, (d) 45°, (e) 60°, and (f) 90°. Scale bars, 5 μm. Schematics of force analysis for ZnO/Au rods. Note the force, F, does not pass through the center of mass (black dot) and induces a torque. Rods moving under (g) perpendicular and (h) parallel light irradiations. The motion mode depends on the torque, T, which is proportional to the force perpendicular to the major axis of the rod, $F_\perp$.

Due to this simple and effective control of the motion modes, the rods are expected to perform complex tasks. Figure 5 shows that the ZnO/Au rod can manipulate cargos by

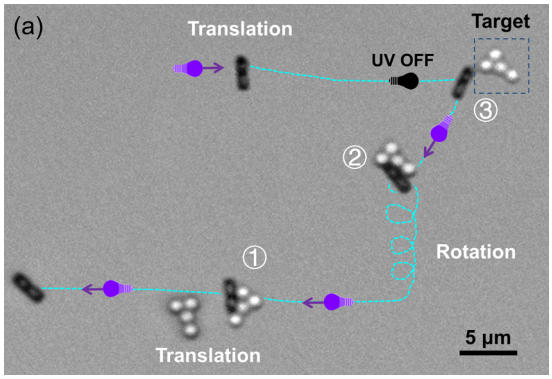

Figure 5. Superimposed time-lapse snapshots of cargos manipulation by ZnO/Au rods. The ZnO/Au rod can ① capture, ② transport, and ③ release cargos by combining translational and rotational motion. The cargos are negatively charged silica microspheres with a diameter of 1.5 μm.

utilizing two modes of motion. Under the parallel UV light irradiation, the rod travels in the translation mode to approach and capture cargos via electrostatic attraction.[40] The rod then transports the cargos to a target location in the rotational mode by tuning the incident angle of the light to 45° (step ②). Finally, the UV light is switched off and the rod releases the cargos due to electrostatic repulsion.[40] The rotation is essential for cargo transportation, as controlled experiments have showed that the ZnO/Au rod can accidentally lose its cargo in translational motion (Supporting Information, Figure S9).

https://dx.doi.org/10.1021/jacs.9b13093
J. Am. Chem. Soc. 2020, 142, 2213–2217

In conclusion, ZnO/Au rods with multiple motion modes have been designed and synthesized. The motion modes include linear translational motion, helical motion, and circular motion. These modes can be switched simply by tuning the H_2O_2 concentration or the incident angle of the light irradiating the rods, resulting from the distinctive and well-defined structural asymmetry of the twinned rods. The various motion modes of ZnO/Au rods demonstrated here can be exploited for the development of model systems for fundamental studies of active matter or for the development of functional micromachines.[41−43]

■ ASSOCIATED CONTENT

Supporting Information

The Supporting Information is available free of charge at https://pubs.acs.org/doi/10.1021/jacs.9b13093.

Supporting figures and experimental details (PDF)

Supporting video S1, showing the effect of H_2O_2 concentrations on the modes of motion of the ZnO/Au rods (AVI)

Supporting video S2, showing how the orientation of incident light dictates the modes of motion of the ZnO/Au rods (AVI)

■ AUTHOR INFORMATION

Corresponding Authors

Wei Wang − *School of Materials Science and Engineering, Harbin Institute of Technology (Shenzhen), Shenzhen 518055, China*; Email: weiwangsz@hit.edu.cn

Zexin Zhang − *College of Chemistry, Chemical Engineering and Materials Science and Center for Soft Condensed Matter Physics and Interdisciplinary Research, Soochow University, Suzhou 215123, China*; orcid.org/0000-0002-4963-5002; Email: zhangzx@suda.edu.cn

Authors

Sinan Du − *Center for Soft Condensed Matter Physics and Interdisciplinary Research and College of Chemistry, Chemical Engineering and Materials Science, Soochow University, Suzhou 215006, China*

Huaguang Wang − *College of Chemistry, Chemical Engineering and Materials Science, Soochow University, Suzhou 215123, China*

Chao Zhou − *School of Materials Science and Engineering, Harbin Institute of Technology (Shenzhen), Shenzhen 518055, China*

Complete contact information is available at: https://pubs.acs.org/10.1021/jacs.9b13093

Notes

The authors declare no competing financial interest.

■ ACKNOWLEDGMENTS

We thank Professor John Brash for critical reading of the manuscript. This work was financially supported by the National Natural Science Foundation of China (Nos. 11574222, 21522404, and 11774075), the Natural Science Foundation of the Jiangsu Higher Education Institutions of China (No. 17KJB140020), and the PAPD program of Jiangsu Higher Education Institutions.

■ REFERENCES

(1) Palacci, J.; Sacanna, S.; Steinberg, A. P.; Pine, D. J.; Chaikin, P. M. Living crystals of light-activated colloidal surfers. *Science* **2013**, *339* (6122), 936−940.

(2) Dong, R.; Hu, Y.; Wu, Y.; Gao, W.; Ren, B.; Wang, Q.; Cai, Y. Visible-Light-Driven BiOI-Based Janus Micromotor in Pure Water. *J. Am. Chem. Soc.* **2017**, *139*, 1722−1725.

(3) Paxton, W. F.; Kistler, K. C.; Olmeda, C. C.; Sen, A.; St Angelo, S. K.; Cao, Y.; Mallouk, T. E.; Lammert, P. E.; Crespi, V. H. Catalytic nanomotors: autonomous movement of striped nanorods. *J. Am. Chem. Soc.* **2004**, *126*, 13424−13431.

(4) Wu, Y.; Si, T.; Gao, C.; Yang, M.; He, Q. Bubble-Pair Propelled Colloidal Kayaker. *J. Am. Chem. Soc.* **2018**, *140*, 11902−11905.

(5) Narinder, N.; Bechinger, C.; Gomez-Solano, J. R. Memory-Induced Transition from a Persistent Random Walk to Circular Motion for Achiral Microswimmers. *Phys. Rev. Lett.* **2018**, *121*, 078003.

(6) Zhang, H.; Duan, W.; Liu, L.; Sen, A. Depolymerization-powered autonomous motors using biocompatible fuel. *J. Am. Chem. Soc.* **2013**, *135*, 15734−15737.

(7) Zheng, J.; Wang, J.; Xiong, Z.; Wan, Z.; Zhan, X.; Yang, S.; Chen, J.; Dai, J.; Tang, J. Full Spectrum Tunable Visible-Light-Driven Alloy Nanomotor. *Adv. Funct. Mater.* **2019**, *29*, 1901768.

(8) Solovev, A. A.; Sanchez, S.; Pumera, M.; Mei, Y.; Schmidt, O. G. Magnetic Control of Tubular Catalytic Microbots for the Transport, Assembly, and Delivery of Micro-objects. *Adv. Funct. Mater.* **2010**, *20*, 2430−2435.

(9) Guo, J.; Kim, K.; Lei, K. W.; Fan, D. L. Ultra-durable rotary micromotors assembled from nanoentities by electric fields. *Nanoscale* **2015**, *7*, 11363−11370.

(10) Zhou, C.; Zhao, L.; Wei, M.; Wang, W. Twists and Turns of Orbiting and Spinning Metallic Microparticles Powered by Megahertz Ultrasound. *ACS Nano* **2017**, *11*, 12668−12676.

(11) Mano, N.; Heller, A. Bioelectrochemical propulsion. *J. Am. Chem. Soc.* **2005**, *127*, 11574−11575.

(12) Vizsnyiczai, G.; Frangipane, G.; Maggi, C.; Saglimbeni, F.; Bianchi, S.; Di Leonardo, R. Light controlled 3D micromotors powered by bacteria. *Nat. Commun.* **2017**, *8*, 15974.

(13) Palacci, J.; Sacanna, S.; Abramian, A.; Barral, J.; Hanson, K.; Grosberg, A. Y.; Pine, D. J.; Chaikin, P. M. Artificial rheotaxis. *Sci.Adv.* **2015**, *1*, e1400214.

(14) Wang, W.; Duan, W.; Ahmed, S.; Mallouk, T. E.; Sen, A. Small power: Autonomous nano- and micromotors propelled by self-generated gradients. *Nano Today* **2013**, *8*, 531−554.

(15) Gao, W.; Dong, R.; Thamphiwatana, S.; Li, J.; Gao, W.; Zhang, L.; Wang, J. Artificial micromotors in the mouse's stomach: a step toward in vivo use of synthetic motors. *ACS Nano* **2015**, *9*, 117−123.

(16) Medina-Sanchez, M.; Schwarz, L.; Meyer, A. K.; Hebenstreit, F.; Schmidt, O. G. Cellular Cargo Delivery: Toward Assisted Fertilization by Sperm-Carrying Micromotors. *Nano Lett.* **2016**, *16*, 555−561.

(17) Kong, L.; Mayorga-Martinez, C. C.; Guan, J.; Pumera, M. Fuel-Free Light-Powered TiO2/Pt Janus Micromotors for Enhanced Nitroaromatic Explosives Degradation. *ACS Appl. Mater. Interfaces* **2018**, *10* (26), 22427−22434.

(18) Soler, L.; Magdanz, V.; Fomin, V. M.; Sanchez, S.; Schmidt, O. G. Self-Propelled Micromotors for Cleaning Polluted Water. *ACS Nano* **2013**, *7*, 9611−9620.

(19) Wu, J.; Balasubramanian, S.; Kagan, D.; Manesh, K. M.; Campuzano, S.; Wang, J. Motion-based DNA detection using catalytic nanomotors. *Nat. Commun.* **2010**, *1*, 36.

(20) Wang, Y.; Fei, S. T.; Byun, Y. M.; Lammert, P. E.; Crespi, V. H.; Sen, A.; Mallouk, T. E. Dynamic Interactions between Fast Microscale Rotors. *J. Am. Chem. Soc.* **2009**, *131*, 9926−9927.

(21) Qin, L.; Banholzer, M. J.; Xu, X.; Huang, L.; Mirkin, C. A. Rational design and synthesis of catalytically driven nanorotors. *J. Am. Chem. Soc.* **2007**, *129*, 14870−14871.

(22) Gibbs, J. G.; Fischer, P. Active colloidal microdrills. *Chem. Commun.* **2015**, *51*, 4192−4195.

(23) Zheng, J.; Wang, J.; Xiong, Z.; Wan, Z.; Zhan, X.; Yang, S.; Chen, J.; Dai, J.; Tang, J. Full Spectrum Tunable Visible-Light-Driven Alloy Nanomotor. *Adv. Funct. Mater.* **2019**, *29*, 1901768.
(24) Wang, W.; Chiang, T. Y.; Velegol, D.; Mallouk, T. E. Understanding the efficiency of autonomous nano- and microscale motors. *J. Am. Chem. Soc.* **2013**, *135*, 10557−10565.
(25) Dong, R.; Zhang, Q.; Gao, W.; Pei, A.; Ren, B. Highly Efficient Light-Driven TiO2-Au Janus Micromotors. *ACS Nano* **2016**, *10*, 839−844.
(26) Kim, K.; Xu, X.; Guo, J.; Fan, D. L. Ultrahigh-speed rotating nanoelectromechanical system devices assembled from nanoscale building blocks. *Nat. Commun.* **2014**, *5*, 3632.
(27) Kummel, F.; ten Hagen, B.; Wittkowski, R.; Buttinoni, I.; Eichhorn, R.; Volpe, G.; Lowen, H.; Bechinger, C. Circular motion of asymmetric self-propelling particles. *Phys. Rev. Lett.* **2013**, *110*, 198302.
(28) Catchmark, J. M.; Subramanian, S.; Sen, A. Directed rotational motion of microscale objects using interfacial tension gradients continually generated via catalytic reactions. *Small* **2005**, *1*, 202−206.
(29) Fournier-Bidoz, S.; Arsenault, A. C.; Manners, I.; Ozin, G. A. Synthetic self-propelled nanorotors. *Chem. Commun.* **2005**, *4*, 441−443.
(30) Xi, W.; Solovev, A. A.; Ananth, A. N.; Gracias, D. H.; Sanchez, S.; Schmidt, O. G. Rolled-up magnetic microdrillers: towards remotely controlled minimally invasive surgery. *Nanoscale* **2013**, *5*, 1294−1297.
(31) Kim, K.; Guo, J.; Liang, Z. X.; Zhu, F. Q.; Fan, D. L. Man-made rotary nanomotors: a review of recent developments. *Nanoscale* **2016**, *8*, 10471−10490.
(32) Wu, Z.; Troll, J.; Jeong, H. H.; Wei, Q.; Stang, M.; Ziemssen, F.; Wang, Z.; Dong, M.; Schnichels, S.; Qiu, T.; Fischer, P. A swarm of slippery micropropellers penetrates the vitreous body of the eye. *Sci. Adv.* **2018**, *4*, eaat4388.
(33) Schamel, D.; Mark, A. G.; Gibbs, J. G.; Miksch, C.; Morozov, K. I.; Leshansky, A. M.; Fischer, P. Nanopropellers and Their Actuation in Complex Viscoelastic Media. *ACS Nano* **2014**, *8*, 8794−8801.
(34) Nicholls, D.; DeVerse, A.; Esplin, R.; Castaneda, J.; Loyd, Y.; Nair, R.; Voinescu, R.; Zhou, C.; Wang, W.; Gibbs, J. G. Shape-Dependent Motion of Structured Photoactive Microswimmers. *ACS Appl. Mater. Interfaces* **2018**, *10*, 18050−18056.
(35) Niu, R.; Kreissl, P.; Brown, A. T.; Rempfer, G.; Botin, D.; Holm, C.; Palberg, T.; de Graaf, J. Microfluidic pumping by micromolar salt concentrations. *Soft Matter* **2017**, *13*, 1505−1518.
(36) Takagi, D.; Braunschweig, A. B.; Zhang, J.; Shelley, M. J. Dispersion of self-propelled rods undergoing fluctuation-driven flips. *Phys. Rev. Lett.* **2013**, *110*, 038301.
(37) Gibbs, J. G.; Zhao, Y. P. Design and characterization of rotational multicomponent catalytic nanomotors. *Small* **2009**, *5* (20), 2304−2308.
(38) Campbell, A. I.; Wittkowski, R.; Ten Hagen, B.; Lowen, H.; Ebbens, S. J. Helical paths, gravitaxis, and separation phenomena for mass-anisotropic self-propelling colloids: Experiment versus theory. *J. Chem. Phys.* **2017**, *147*, 084905.
(39) van Teeffelen, S.; Lowen, H. Dynamics of a Brownian circle swimmer. *Phys. Rev. E* **2008**, *78*, 020101.
(40) Wang, W.; Duan, W.; Sen, A.; Mallouk, T. E. Catalytically powered dynamic assembly of rod-shaped nanomotors and passive tracer particles. *Proc. Natl. Acad. Sci. U. S. A.* **2013**, *110*, 17744−17749.
(41) Karshalev, E.; Esteban-Fernandez de Avila, B.; Wang, J. Micromotors for "Chemistry-on-the-Fly". *J. Am. Chem. Soc.* **2018**, *140*, 3810−3820.
(42) Dong, R.; Cai, Y.; Yang, Y.; Gao, W.; Ren, B. Photocatalytic Micro/Nanomotors: From Construction to Applications. *Acc. Chem. Res.* **2018**, *51*, 1940−1947.
(43) Zhang, J.; Luijten, E.; Grzybowski, B. A.; Granick, S. Active colloids with collective mobility status and research opportunities. *Chem. Soc. Rev.* **2017**, *46*, 5551−5569.

https://dx.doi.org/10.1021/jacs.9b13093
J. Am. Chem. Soc. 2020, 142, 2213−2217